IAC-03-A.P.22

Automated Star Sensor Performance Assessment using Real-Sky Data of MEFIST II

M. Kruijff*, N. v.d. Heiden+

* Delta-Utec Space Research and Consultancy, Leiden, the Netherlands, www.delta-utec.com
TNO-TPD, Delft, the Netherlands, www.tpd.tno.nl

Abstract

This paper reports on the testing of a novel tool for batch processing of star sensor imagery and camera performance and design assessment.
Star sensors based on pattern recognition provide the most accurate attitude solution available for spacecraft, even when using large field of view cameras. Due to advances in CCD, CMOS, integrated circuit technologies, and robust algorithms, star sensors are becoming more and more a viable alternative to solutions that were traditionally cheaper. A great many star sensor hardware is thus currently under development worldwide. This trend creates a market for generic design support software, automated batch processing of imagery resulting from real-sky tests and automated camera performance assessment.
For this purpose, the Attitude Determination Test Environment (ADTE) tool was developed (formerly known as SSATT). The major novelty of the ADTE is that it contains a generic interface to batch process real-sky test imagery that provides as output the average directional accuracy of the camera, lens deviation correction estimates and performance distributions as a function of star magnitude or star class. No sophisticated test set-up or idealized mathematical performance analysis is necessary. The tool includes camera simulation settings and up-to-date detection/rejection, centroiding and pattern recognition algorithms including upgraded versions of Liebe, Quine and Delta-Utec Douma Extension (DUDE). Pattern data storage and retrieval is based on the very fast multidimensional pointer-based array algorithms. Various recursive validation techniques maximize the number of recognized stars per image.
The ADTE tool was first used for the real-sky test of the MEFIST-II camera in the Negev desert. This paper shortly explains the functionality of the tool and algorithms behind it and focuses on the analyses and results performed for MEFIST-II.

1. ADTE functionality

The Attitude Determination Test Environment (ADTE) is a tool for:

- Star sensor camera hardware development (requirements definition, performance estimation etc.).
- Star sensor algorithm development (test bed via dll interface).
- Assessment of performance of real-sky imagery.
- Variety of spin-off applications

A full set of advanced algorithms has been developed for ADTE, that have shown to be very generic and can be used with any star sensor as well as with many ground applications.

Major functionality:

- Star catalogue conversion (selection of suitable stars, conversion from visual to instrumental magnitude)
- Automated star-triangle database production for embedded (flight) system (on-board database)
- Unique database organization for immediate star identification with (near-) zero search time
- Input of real images or fast graphic simulation of camera images (for Monte Carlo simulation of the full sky, including camera-specific noise, Fig. 1.1)
- Star detection/centroiding
- Star-triangle recognition and validation algorithms
- QUEST attitude determination

Further features:

- Dealing with complications such as optical-binary stars, false star rejection etc.
- Genetic algorithm optimization of lens projection
- Interface with TNO-TPD developed synthetic image generator (noisy star pixel maps)
- Flight software version (embedded system C++ code) of the image processing, star identification and attitude determination

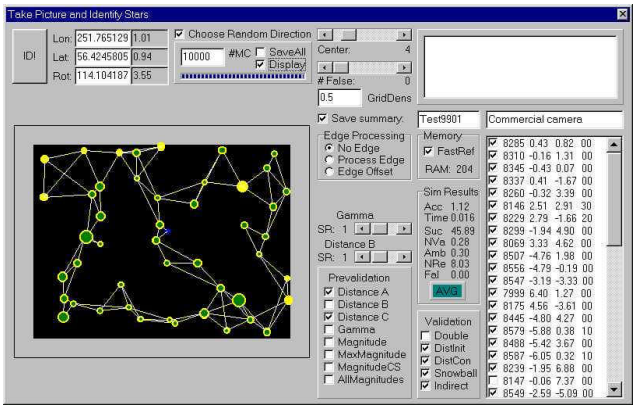

Fig. 1.1 ADTE Image Recognition Screen

2. Algorithms of ADTE

This section gives a brief overview of the star identification algorithms that are explained in detail in [Ref. 2], as well as the detection, rejection and centroiding algorithms.

In ADTE, the star recognition from a CCD image is performed by extracting, for each star to-be-identified, a combination of features of a triangular pattern.

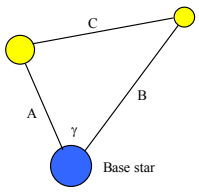

Fig. 2.1: A triangle pattern plus feature definitions

Useful features must be independent from the camera attitude and can thus be a magnitude or a great-circle angular distance between two stars (see Fig. 2.1).
In ADTE, any combination of the above can be used for identification. When a triangle pattern's features have been measured in the image, a database is searched for a very similar pattern that is used for identification. Using a pointer based search strategy and a uniformized database, all candidate triangles are located in a single step, completely independent of the database size.
After recognition, to achieve the required reliability, the candidate identifications need to be filtered through a validation algorithm. Various algorithms are available.
With a group of stars identified, the Star Sensor Algorithm Test Tool applies the QUEST algorithm[4,5] to obtain an attitude estimate and investigate performance.

3.2 MEFIST II real sky tests

The MEFIST II star sensor camera is a development by TNO-TPD in Delft, The Netherlands (Figure 3.1). ADTE was used to investigate over a 1000 images, taken in the Negev desert on 5-6 July 2000 (Fig. 3.12). Latitude of the observation site was about 31 degrees. The camera was pointing zenith, so this is also the latitude of the starsky in the images. Celestial longitude ranged from ~270-320 degrees, increasing with time at 15 degrees/hour. This change in longitude due to rotation of the Earth could be accurately reconstructed from the attitude solutions of the series of images, taken at 15 s interval. At regular intervals (every 120 images) rotation of ~20 degrees was performed, total clockwise rotation varied from 3 to 84 degrees. Table 3.3 provides an overview of the cases studied.

Image case	*Number of images studied*
800-8, 4 rotations*	479
800-4, 1 rotation	109
400-4, 4 rotations	473
Rate 200-8 (3 deg/6 deg)	60
Moon 100-1, 500-2, 500-4, 800-2	43 (number available, a selection was studied)

Table 3.3: explanation of cases: 800-8, 4 rotations: Integration time **800** ms, programmable gain set to **8**. Camera was oriented to zenith, and rotated **4** times around boresight axis

Reference case was the 800 ms integration time, gain setting "8". This is theoretically the most sensitive case, and therefore possibly the most accurate. It should be noted that the integration time of 800 ms causes a blur of 10.4 arcsec, or 0.055 pixel (each pixel = 188 arcsec), which might degrad static performance a bit.
Effect of gain and integration time were to be studied from the other settings with abundant imagery: 800-4 and 400-4. Images were studied that were taken with the camera mounted on a pendulum, as a means of rate simulation. Finally some special attention was reserved for images with the moon in the FOV, to verify problemless centroiding in the presence of large amounts of noise.
The camera electronics have removed the majority of the dark current noise from the images, so the noise level on all images seems very low.

Figure 3.1 shows the positions of all reliably identified stars in the FOV of the camera combined for all 800-8 images giving an impression of the spatial coverage of the CCD that was taken into account for the various performance estimates. Individual stars generally appear on subsequent images at slightly shifted location, hence the "strikes" in the image. Fig 3.2 shows for the same settings and the same stars the spatial coverage over the celestial sky.

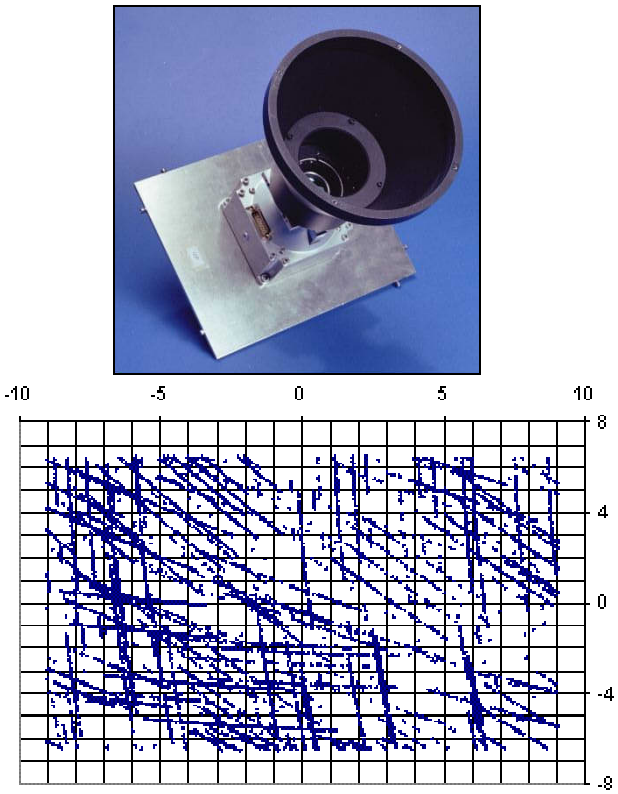

Figure 3.1: above: MESIFT II. Below: position of all identified and accepted stars in the FOV of the camera combined for all 800-8 images. The apparent stripes indicate the shift of individual stars within the FOV, due to slow motion of the zenith (and camera) through the sky due ot rotation of the Earth. The Earth rotation could be calculated back with high precision from this data. Identified stars near the edge of the screen are rejected because they have higher likelihood of being false and have less precision due to projection of the lense.

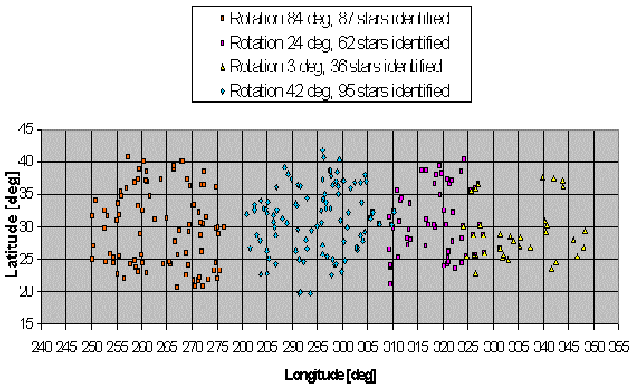

Figure 3.2: Position of the same identified stars as Fig. 3.1, but projected in the celestial sky. The four rotations are indicated by different colors. It will be shown in this paper that the observed reduction in stars identified with increasing longitude is due to reduction in bright star density in the sky.

3.2.1 Determining ADTE camera settings

In order to create an optimal triangle database for a specific camera, the magnitude threshold of the camera needs to be decided. This can be done by experimenting with the setting of the detection threshold for a star's max pixel value, and the number of pixels that is minimally required to build up a star. By using more pixels around the brightest one for each star, one can, to a certain limit, improve centroiding accuracy. The MEFIST is designed for a star spotsize of 3x3 pixels and indeed, the best centroiding results were obtained for about 9 pixels per star. Raising this number to 25 did not result in significant increase in number of identified stars. However, many stars will not be bright enough to light up 9 pixels above the threshold. Therefore, smaller star groups will also be accepted as potential stars.
In below figure 3.3, with 5-6 pixels required and a detection threshold for the brightest pixel value of a star of at least 23, it can be seen that the magnitude threshold should be put to about 6. About 60 stars per image will be found. If 4 pixels are accepted and a detection threshold of 7 pixel value, about 90 stars are found, the weakest of which will have a magnitude of ~6.7. If the detection threshold is set lower, groups of noise pixels surrounding singled-out bright pixels result in a significant number of false stars. Note one can indeed find in Fig. 3.3 that most stars light up about 8-9 pixels.

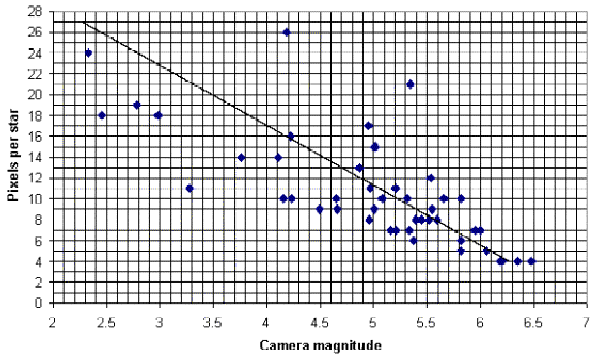

Figure 3.3: Relation between star size in pixels (above treshold) and camera magnitude. Data from 07052258.b00

The conclusion that most stars take up about 9 pixels is reinforced by studying Figure 3.4. It shows the collected distances of pixel centers to the centroids of the stars they surround. It only includes the pixels from stars with a magnitude over 5.0. A nice Gaussian distribution is recognized for these most common (weak) stars. Their average projected size can be estimated to be of diameter ~3.5 pixel, again quite as expected, i.e. between the inner circle of a 3x3 pixel area (diameter 3) and its outer circle (diameter 4.2), therefore covering about 9 pixels in all.
Brighter stars do not quite follow this shape and there is evidence of blooming (bulging out of bright pixels at relatively large distance to the centroid; flat upper limits in pixel brightness can be distinguished representing local blooming limits). The bloom limits vary, between 150 and 220 (due to local-noise reduction by the camera hardware this value is not 255 as may be expected for a one-byte signal).

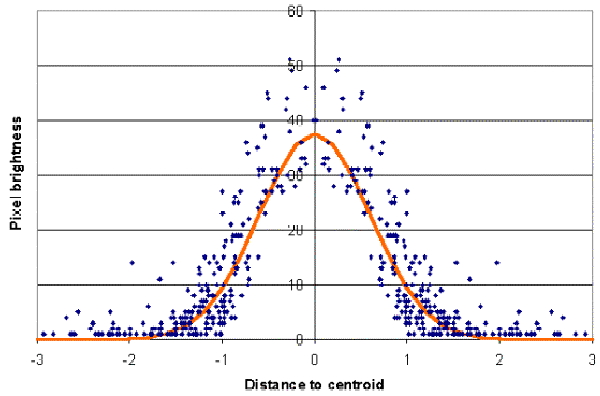

Figure 3.4 Distance of pixel center to centroid of star. Stars weaker than Magnitude 5. Data from 07052258.b00 (Red curve is a Gaussian curve with 1 sigma=0.6)

The identification performance of the ADTE algorithms was somewhat limited because only the Yale's Bright Star Catalogue was available, with 9096 stars complete to magnitude 6, rather than the camera's magnitude 6.7 established sensitivity. To match the catalogue, camera threshold was conservatively set to 5.7. The triangle-database-creation algorithm also needs the Centroiding Error (CE), which was found to be about ~40-55 arcsec. DUDE was the algorithm of choice.

During the star identification process the 2D-database is searched for candidate triangles with matching angles A and C (Fig. 2.1), before further validation is performed.

3.2.2 Magnitude reconstruction performance

Star magnitude is a logarithmic expression of brightness. Therefore, if all of a star's 9 pixelvalues are summed, it would ideally follow a straight line on a logarithmic plot, with slope -2.5. The offset is to be determined by a best fit of a line with such a slope. The observed data fits to a line of slope -2.17 (Fig. 3.5). The slight difference could have something to do with the clipping of pixel values by the noise reduction hardware inside the camera. This process affects relatively more the pixel summation for weak stars than it does for bright ones, shifting stars with high magnitude more to the lower summations, in Fig. 3.5. Bright star magnitude could be underestimated due to blooming. Sticking to generality, a best fit with slope –2.5 was enforced.

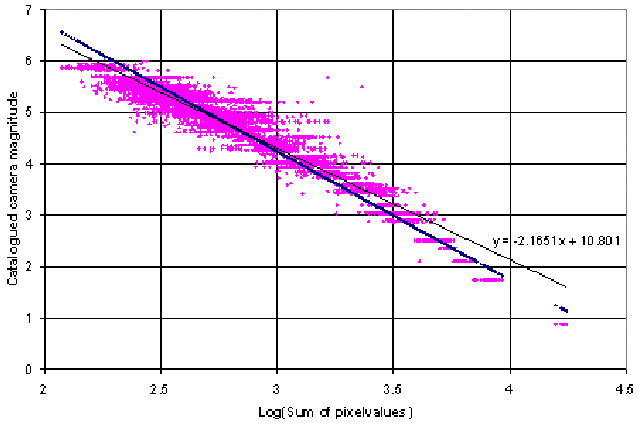

Figure 3.5: Logarithm of summation of an identified star's pixelvalue as a function of its catalogued camera magnitude. Two fits are shown, a best fit (slope –2.17) and a fit with enforced ideal slope (-2.5). The difference is not very significant but can be explained by the camera hardware functioning.

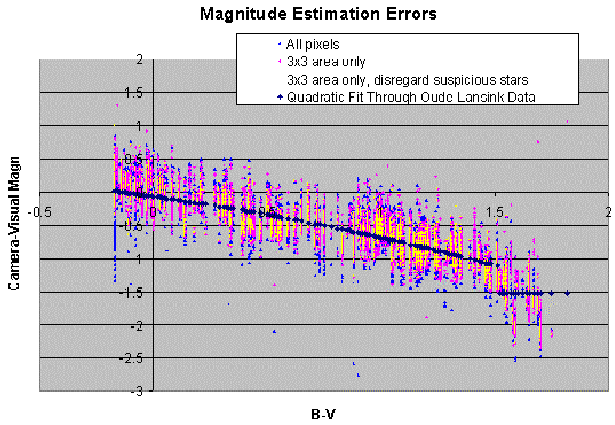

Figure 3.6: ADTE camera magnitude reconstruction of identified stars as compared to predictions from catalogue data (compare Fig. 2.2).

Remember that the catalogue only provides visual magnitudes. The conversion to camera magnitude for MEFIST was determined before the test from a calibration set by Oude-Lansink at TNO-TPD[2].

Figure 3.6 shows how well the reconstruction of camera magnitudes from the pixel summations match Lansink's predicted quadratic curve. Star camera magnitudes can thus be well predicted based on the catalogued (visual) data. This allows for ADTE to create a near-optimal database, beneficial to identification performance:

the star magnitude noise affects the likelihood of certain triangles to occur. The 1 sigma magnitude error of Lansink's quadratic fit is 0.17 [2]. The final magnitude estimation noise during the real-sky test ranges from 0.2-0.23 for an assumed 3x3 pixel star size.

3.2.3 Lens adjustment model

To obtain the best possible attitude reconstruction, a 1-dimensional lens projection adjustment model was provided by TNO-TPD and included into the image-to-sky coordinate transformation[12]. We further detailed it, in 2D, using ADTE's optimization algorithm in the following manner.

20 Well-identified images were selected from the g8-i800 dataset, covering all 4 rotational angles and a representative selection of celestial longitudes. From each of these images, 15 stars were selected, all in all giving a more or less equally distributed coverage over the FOV or lens projection area (Figure 3.7). A cost function was set-up, adding all squared distance errors (difference between centroided and catalogued angular distance) between all possible pairs of selected stars within a single image. This cost was minimized through genetic algorithm optimization[11], in a variety of parameter ranges. A typical lens projection adjustment result is given in

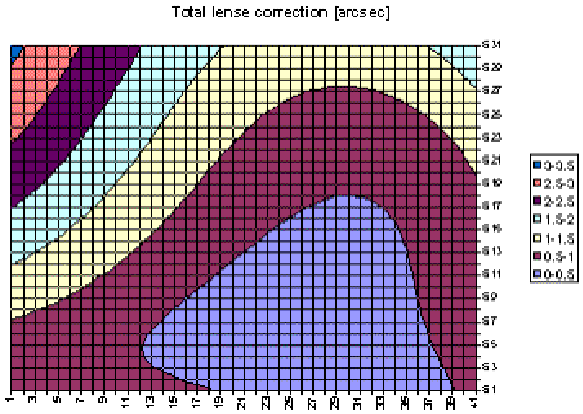

Figure 3.8. The genetic algorithms were run over a relatively small number of generations (1000), and considerable improvement might as yet be possible. However, a consistent improvement in attitude performance (~40%) was already noticed.

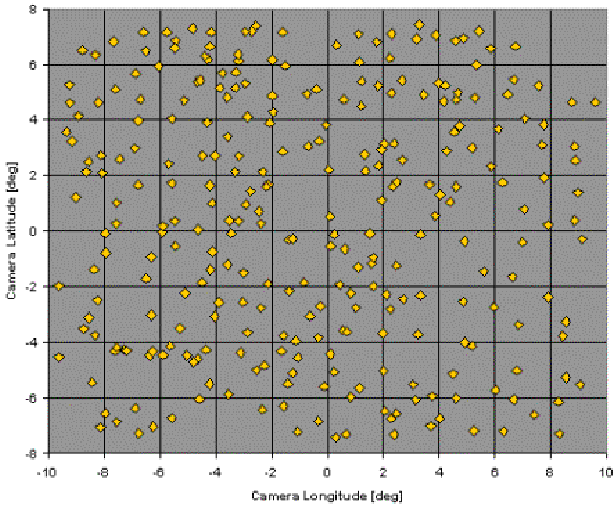

Figure 3.7: Position of selection of 300 reliably-identified stars in the FOV of the camera taken from 800-8 images. It was attempted to obtain a uniform distribution.

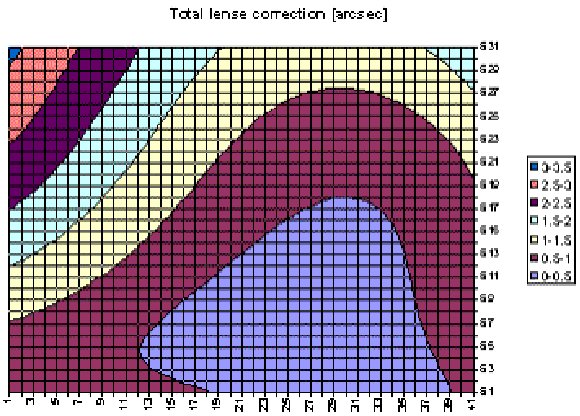

Figure 3.8: Magnitude of centroiding adjustments with respect to ideal lens, determined by Genetic Algorithms. The grid should be overlaid with the CCD surface. The axis numbering is in an awkward scale, derived from Excel column/row number, i.e. (half degrees+1) measured from the corner of the CCD.

3.2.4 Attitude reconstruction performance

As there is no reference attitude for the images two methods have been used to determine the attitude accuracy. The methods are referred to as the *latitude method* and the *cloud method*.

The latitude method is based on the principle that during a test (same setting, same rotation) the camera points straight up in the same direction and therefore the reconstructed latitude should stay constant. However due to atmospheric effects and possible tiny displacements of the tripod due to wind and or temperature effects this assumption is only valid within a few arc seconds accuracy. In some cases a clear and consistent drift was observed of the latitude direction of several arcsec per minute. It is also possible that this drift is due low frequency changes within the camera hardware, but due to lack of reference attitude, it is not possible to distinguish between these drifts. We have to limit ourselves to quantify the attitude reconstruction noise with respect to the momentary (unknown) offset. Drift effects are thus to be removed. We therefore fit a second order polynomial through the latitude deviations from the average reconstructed attitudes. To obtain a measure for the reconstruction accuracy, the deviation to this fit is multiplied by $\sqrt{2}$. This accounts for identical and independent error in longitude direction. In Fig. 3.9 an example is presented for the g4-i800 photo series. The blue dots represent the latitude deviation from the average reconstructed latitude in this photo series. Through these blue dots a trend-line is fitted. The quoted accuracy is 10.6 arcsec is $\sqrt{2}$ * the standard deviation around this trend.

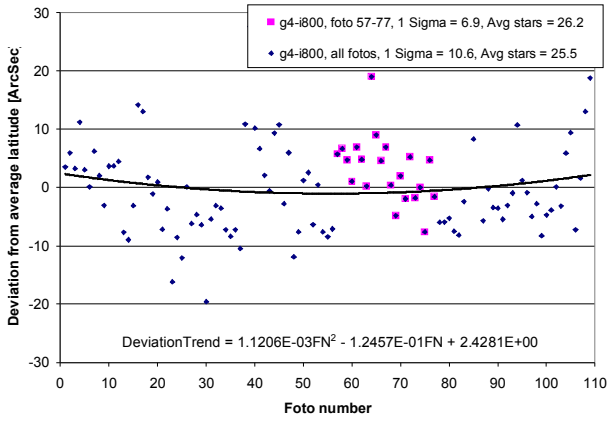

Fig. 3.9: Latitude method for attitude reconstruction. The actual camera orientation's latitude is assumed to change only slowly over time, as consecutive images are taken during the testing. Noise around the trendline can be interpreted as a way to determine the 1D-attitude reconstruction error. This simple method works surprisingly well.

The cloud method (Fig. 3.10) reconstruction accuracy is obtained by multiple attitude reconstructions of a selected image (bootstrap method). Each attitude reconstruction is performed with a different subset of identified stars, roughly representing the range of performance through out all the tests. The deviation of each reconstructed attitude with respect to the average attitude is then scaled to the average number of stars of the originally identified set. The scaling is performed in order to correct for the number of stars used for each attitude reconstruction. As the attitude reconstruction accuracy is inversely proportional to the square root of the number of stars used for the attitude reconstruction the applied scaling for each deviation equals $\sqrt{}$(number of stars used to reconstruct attitude)/ $\sqrt{}$(average number of stars of original identification). The standard deviation of these scaled errors is the measure for the reconstruction accuracy with the cloud method.

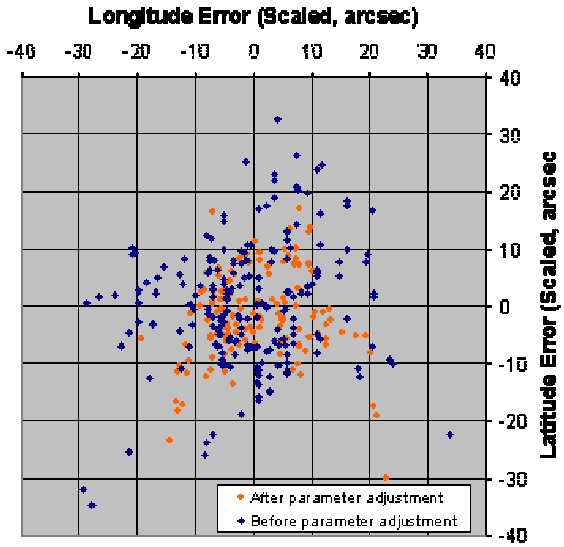

Fig. 3.10: Cloud method for attitude reconstruction. Attitude is reconstructed using different subsets of the set of identified stars for a certain image. The errors with respect to the average direction are plotted (bootstrap method). This method gives no insight into the offset, e.g. due to misalignments, but gives good insight into the standard deviation of the reconstruction. Two sets are plotted, the orange one is after parametric lens adjustment and significantly improves performance.

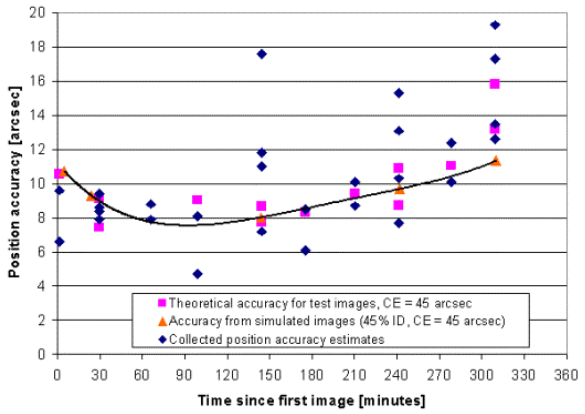

Fig. 3.11: Attitude reconstruction error estimates over time. The performance change with (test) time can be explained by the change of star density in the sky due to Earth rotation. See text for explanation.

Both methods give comparable results (the results combined are plotted with blue diamonds in Fig. 3.11). The number of stars in the sky changes due to rotation of the Earth. Therefore the obtainable accuracy changes with time, roughly according to *Centroiding Error / √ (0.45 x number of stars in simulated image)*. This formula takes into account that the average number of stars used for attitude determination with current settings is about 45% of the total amount of stars in the image. Whereas the blue diamonds indicate the combined estimates of the two methods using real-sky images, the pink squares are performance calculated with above formula, for the same number of stars that ADTE identified in the real-sky images. A centroiding error of 45 arcsec is assumed (0.24 pixel). We also created with ADTE fully simulated images for the same directions and let ADTE reconstruct attitude, assuming centroiding error of 45 arcsec. The curve (with red triangles) indicates the results.
Both theoretical results show the same trend as the results obtained by the test series, suggesting that the source of the tendency is merely the number of stars in FOV. The dominant effect of the number of stars on the attitude reconstruction error makes it impossible to determine effects of camera settings and or temperature effects.

In conclusion: attitude reconstruction precision for MEFIST II is thus found to be about 10 arcsec. Some improvements may be expected.
In space there will be no atmospheric noise & absorption/reflection effects, also extra precision may be gained by using a more complete star catalogue for the g8-i800 setting. Centroiding error can be improved: lens correction was not fully optimized (i.e. convergent), merely a general improvement of performance was achieved. Rotation of the Earth during the tests may have accounted for 5-10 arcsec contribution.

Note that we adopted in this document the term Attitude Reconstruction Precision (ARP) rather than the Noise Equivalent Angle (NEA). NEA is defined as[9]:
"The star tracker's ability to reproduce the same attitude when it is continously presented with the same star image. NEA is a nonsystematic, or random error component."
It is expected that the average of the ARP found by the two methods is a good representation of the NEA. In the definition of NEA, the ARP via the latitude method would give an upper limit of the NEA (because of the timeframe of 1 hour of a test series). On the other hand the cloud method would give a lower limit of the NEA because it is based on exactly the same camera image rather than the same star image.

3.2.5 Reliability of ADTE attitude reconstruction

Success is defined as: fraction of successfully identified images out of all images.
Reliability is defined as: fraction of successfull identified images out of all identified images.
Reliability is considered more important, since it is not so bad to skip a datapoint in a sequence of attitude estimations, but it is bad if an attitude is passed on, though wrong.

Reliability is always found to be 100%. False attitudes always have a warning tag (too little pixels, suspected double star, edge of screen etc.). In the way to deal with warning tags, we distinguish two options:

- Strict recognition
- Non-strict recognition

In case of a strict recognition (rejecting all stars with warning tag), only 0.2% of the images (i.e. one) yielded a wrong attitude, but it included a warning tag. 14 Images did not yield an attitude at all. So *success* for strict recognition can be estimated at 97%.

Non-strict recognition also rejects stars with warning tags, but allows them to participate if too little reliable stars are available. Images with only 3 identified stars are rejected no matter what. For non-strict recognition the *success* fraction is 99%. Reliability is still 100%.

Fig. 3.12 Installation of MEFIST on Wise Observatory, Negev desert.

Conclusions

The ADTE star sensor test environment was successfully applied to the real-sky images produced by TNO's MEFIST II star sensor in the Negev desert. Over a 1000 images were batch processed, resulting in a measure for the camera's accuracy (better than 10 arcsec), reliability (97%) and success rate (99%). The ADTE centroiding algorithms performed at 45 arcsec per star. Consistently, 45% of the stars in the image were identified, all correctly. Magnitude reconstruction precision was better than 0.24, compared to a theoretical maximum obtainable accuracy of 0.17. Independent measures for attitude reconstruction accuracy demonstrate that estimates are consistent with theory and that trends in variations in performance can be mostly ascribed to the number of stars that are in fact inside the field of view.

Acknowledgments

The MEFIST-II testing was performed under Dutch NRT-2802T funding with TNO-TPD, with support of University of Tel Aviv and Asher Space Research Institute (ASRI), from the Technion University in Haifa.

References

[1] Liebe, C.C., "Star Trackers for Attitude Determination", IEEE AES Systems Magazine, June 1995.

[2] Heide, E.J., Kruijff, M., Oude-Lansink, D., Douma, S., Development and Validation of a Fast and Reliable Star Sensor Algorithm with Reduced Database, IAF-98.A.6.05, available from www.delta-utec.com.

[3] Zuiderwijk, S., Kruijff, M., Heide, E.J. v.d., "ADTE: A Tool for Automated Evaluation of Star Sensor Design, Performance and On-Board Algorithms". 4th ESA International Conference on Spacecraft Guidance, Navigation and Control Systems, ESTEC[i]. , Noordwijk, 18-21 October 1999, ESA-SP-425, February 2000

[4] Shuster & Oh, Three Axis Determination from Vector Observations, JGC, AIAA81-4003

[5] Bar-Itzhack, I.Y., "REQUEST: A Recursive QUEST Algorithm for Sequential Attitude Determination", AIAA Vol 19, Number 5, pages 1034-1038

[6] Douma, S.R., "Development of an Algorithm for Autonomous Star Identification", Delft University of Technology, Faculty of Aerospace Engineering, 1997

[7] Bezooijen, R.W.H., "Automated Star Pattern Recognition", PhD Stanford University, California 1989

[8] Quine, B.M., Durrant-Whyte, H.F., "A fast autonomous star acquisition algorithm for spacecraft, In proceeding of IFAC Autonomous Control Conference", Beijing, 1995

[9] Eisenman, A, Liebe, C.C, The advancing State-of-the-Art in Second Generation Star Trackers, JPL

[10] Zuiderwijk, S., The Star Sensor Control Unit, An embedded solution for autonomous attitude determination, Hogeschool van Utrecht/Delta-Utec, May 2000.

[11] Biesbroek, R., Evolution in a Micro-Chip, A Brief Study into Genetic Algorithms ESA/ESTEC working paper, E.W.P. 1870, 1996.

[12] Heiden, N. v.d., TNO TPD Medium Field Star Tracker (MEFIST) performance. TPD-NRT-MEFIST-TN-01, June 2000

[13] M. Kruijff, E.J. van der Heide, Image Processing for MEFIST Real Sky Test Negev Desert - July 2000. Delta Utec, May 2001.